

Continuous wave and active *Q*-switched operation of Watt-level LED-pumped two-rod Nd,Ce:YAG laser

Jian-Ping Shen(沈建平), Peng Lu(芦鹏), Shao-Cong Xu(徐少聪), Rong-Rong Jiang(江容容), Yang Chen(陈阳), Liang Chen(陈亮), and Feng-Yang Xing(邢凤阳)

Citation: Chin. Phys. B, 2024, 33 (**7**): 074207. DOI: 10.1088/1674-1056/ad34c9
Journal homepage: http://cpb.iphy.ac.cn; http://iopscience.iop.org/cpb

What follows is a list of articles you may be interested in

Wavelength switchable mode-locked fiber laser with a few-mode fiber filter

Shaokang Bai(白少康), Yujin Xiang(向昱锦), and Zuxing Zhang(张祖兴)
Chin. Phys. B, 2023, 32 (**2**): 024209. DOI: 10.1088/1674-1056/ac744f

Watt-level, green-pumped optical parametric oscillator based on periodically poled potassium titanyl phosphate with high extraction efficiency

Hang-Hang Yu(俞航航), Zhi-Tao Zhang(张志韬), and Hong-Wen Xuan(玄洪文)
Chin. Phys. B, 2022, 31 (**12**): 124203. DOI: 10.1088/1674-1056/ac8346

High-sensitivity methane monitoring based on quasi-fundamental mode matched continuous-wave cavity ring-down spectroscopy

Zhe Li(李哲), Shuang Yang(杨爽), Zhirong Zhang(张志荣), Hua Xia(夏滑), Tao Pang(庞涛),Bian Wu(吴边), Pengshuai Sun(孙鹏帅), Huadong Wang(王华东), and Runqing Yu(余润磬)
Chin. Phys. B, 2022, 31 (**9**): 094207. DOI: 10.1088/1674-1056/ac5d33

Pump pulse characteristics of quasi-continuous-wave diode-side-pumped Nd:YAG laser

Zexin Song(宋泽鑫), Qi Bian(卞奇), Yu Shen(申玉), Keling Gong(龚柯菱), Nan Zong(宗楠), Qingshuang Zong(宗庆霜), Yong Bo(薄勇), and Qinjun Peng(彭钦军)
Chin. Phys. B, 2022, 31 (**5**): 054208. DOI: 10.1088/1674-1056/ac447f

Different supercontinuum generation processes in photonic crystal fibers pumped with a 1064-nm picosecond pulse

Chen Hong-Wei (谌鸿伟), Jin Ai-Jun (靳爱军), Chen Sheng-Ping (陈胜平), Hou Jing (侯静), Lu Qi-Sheng (陆启生)
Chin. Phys. B, 2013, 22 (**8**): 084205. DOI: 10.1088/1674-1056/22/8/084205

Continuous wave and active *Q*-switched operation of Watt-level LED-pumped two-rod Nd,Ce:YAG laser

Jian-Ping Shen(沈建平)[†], Peng Lu(芦鹏), Shao-Cong Xu(徐少聪), Rong-Rong Jiang(江容容), Yang Chen(陈阳), Liang Chen(陈亮), and Feng-Yang Xing(邢凤阳)

College of Electronic and Optical Engineering & College of Flexible Electronics, Nanjing University of Posts and Telecommunications, Nanjing 210023, *China*

(Received 29 January 2024; revised manuscript received 10 March 2024; accepted manuscript online 18 March 2024)

A high-performance LED-side-pumped two-rod Nd,Ce:YAG laser with continuous-wave (CW) and acousto–optical (A-O) *Q*-switched operation is demonstrated in this work. A symmetrically shaped flat–flat cavity with two identical LED-side-pumped laser modules is employed for power scalability. In the CW regime, the maximum output average power of laser at 1064 nm is 4.41 W, corresponding to a maximum optical conversion efficiency of 5.3% and a slope efficiency is 12.4%. In the active *Q*-switched regime, the pulse energy of laser reaches as high as 0.89 mJ at a repetition rate of 800 Hz with a pulse width of 457.2 ns, the corresponding highest peak output power is 1.94 kW and the M^2 factor is measured to be about 8.8. To the best of the authors' knowledge, this is the first demonstration and the highest performance of a CW LED-side-pumped two-rod laser Nd,Ce:YAG with Watt-level output reported so far.

Keywords: Watt-level, LED-pumped, CW, Nd,Ce:YAG, actively *Q*-switched operation

PACS: 42.55.–f, 42.55.Ye, 42.55.Xi, 42.60.Gd **DOI:** 10.1088/1674-1056/ad34c9

1. Introduction

In recent years, the radiant intensity of commercial light-emitting diodes (LEDs) has been elevated to the Watt level per spherical degree (W/Sr), while the application cost has decreased with the development of the lighting and display industries. Meanwhile, in a typical single-color LED, the radiation spectrum has meticulously designed to excite various solid-state media within narrow absorption bands, bringing exceptional performance of high average power and high beam quality to LED-pumped laser oscillators.[1–6] The latest research has successfully demonstrated the operational efficacy of LED-array-pumped solid-state lasers, presenting significant advancements in this field. Particularly, Nd^{3+}-doped materials were directly pumped by NIR LEDs at different peak wavelengths, including 750 nm,[7] 810 nm,[8,9] and 850 nm.[10] And based on the absorption band of Ce^{3+} centred at 460 nm, Nd,Ce:YAG[11] and Ce:YAG[12] were pumped by blue LEDs. In addition, passive[13,14] and active *Q*-switched[15,16] laser demonstrations were also available. However, due to the limitation of LED Lambertian emission, as a pump source, the work efficiency is still inefficient compared with laser diodes (LDs). Additionally, it is imperative to consider the thermal constraints and application features when operating high-power LED arrays in a quasi-continuous wave (QCW) operation, rather than in a CW mode, to achieve the desired high average power LED-pumped solid-state lasers. Therefore, obtaining CW laser output and large mode size lasers using high-power CW LED pumping has been a significant challenge.

Until now, no relevant scientific researches and technical schemes have reported the CW operation of an Watt-level actively *Q*-switched LED-pumped Nd,Ce:YAG / Nd:YAG module. Only a very few scientific achievements have reported LED-pumped Nd:YAG slab CW laser with a maximum output power of 0.37 W by using a thermal-isolated and light-guided experimental configuration,[17] which means that further research and development are required to overcome these limitations and explore the full potential of LED-pumped CW solid-state lasers.

In this work, we are to elucidate a multitude of the issues involved with high-power CW LED pumping laser system. Firstly, LED arrays with a pentagonal shape around the rod are utilized to obtain a sufficient pumping power density, which significantly increases the requirement for the heat dissipation capacity of the heat sink. Secondly, an LED-side-pumped two-rod Nd,Ce:YAG laser structure is designed to reduce the oscillating laser threshold and increase the cavity pump power density. Thirdly, a combination of fine-tuning pump structures, efficient cooling solutions, and laser-gain media characteristics are continuously improved to achieve CW operation of LED-pumped lasers with high average power and high conversion efficiency. Finally, in the CW regime, a maximum average power of 4.41 W at 1064 nm is obtained, corresponding to the highest optical conversion efficiency of 5.3% and a slope efficiency of 12.4%. Furthermore, in the active *Q*-switched regime, the pulse energy of laser reaches as high as 0.89 mJ at a repetition rate of 800 Hz with a pulse width of 457.2 ns, its corresponding highest peak output power is 1.94 kW and the M^2 factor is measured to be about 8.8.

[†]Corresponding author. E-mail: jianpingshen@njupt.edu.cn

© 2024 Chinese Physical Society and IOP Publishing Ltd

2. Experiments setup

The CW LED-side-pumped two-rod Nd,Ce:YAG laser experimental configuration is shown schematically in Fig. 1(a). Firstly, a symmetrically shaped flat–flat cavity employing two identical side-pumped modules was utilized to achieve CW laser power scalability. Secondly, in each pump module, five rows of LED stacked arrays (20 LEDs in each stacked array) were devised in a pentagonal arrangement around the quartz tube to homogenize the pumping distribution and reduce the thermal effect of the crystal rod as shown in Fig. 1(c). An Nd,Ce:YAG rod (Jing Jiu crystal, 5-mm diameter, 120-mm length, Nd^{3+}:1.0 at.%, Ce^{3+}:0.05–0.1 at.%) and an Nd:YAG rod (Dong Jun crystal, 5-mm diameter, 120-mm length, Nd^{3+}:1.0 at.%) were installed in a flow tube with 20-°C cooling-water to provide a suitable environment for 1064-nm excitation contrast experiment. Thirdly, figure 1(b) shows the construction of the 1064-nm all-solid-state laser for Q-switched operation, in which the system consists of two LED-side-pumped Nd,Ce:YAG modules connected in series, an A-O Q-switch and the resonant cavity. A 1064-nm A-O Q-switch (Gooch & Housego. I-QS027-5C4G) was positioned near the output mirror M2. It was driven by a radio frequency (RF) generator (QSD5027) operating at a center frequency of 27.12 MHz and providing a maximum value of RF power of 50 W, thereby generating laser pulses. After that, the resonant cavity was formed by a rear mirror M1 ($R > 99.9\%$@1064 nm) and an output plane coupler M2 ($T = 1.5\%$, 3%, and 5%@1064 nm). The overall CW LED-side-pumped two-rod Nd,Ce:YAG cavity length was approximately 340 mm and the Q-switched laser cavity length was about 400 mm. In the end, a programmable power supply (MH150-30DM-II) with dual channel outputs was employed to ensure that the power supply parameters of both modules were identical and triggered simultaneously. Due to the fact that the sustained operation at absolute maximum currents can result in the excessive junction temperatures and a reduction of device lifetime, the total input current was set to 3 A for each parallel LED stack array corresponding to a maximum value of pumping power of 84 W. Each LED array had a separate heat sink with an internal coolant temperature of 5 °C to ensure that the spectral emission peak of the LED array is shifted to 808 nm, thus improving pumping efficiency. It worth noting that a thermally-electrically separated copper substrate with a higher thermal conductivity (380 W/mK) has replaced the original aluminum substrate in order to optimize the heat dissipation of the insulation layer.

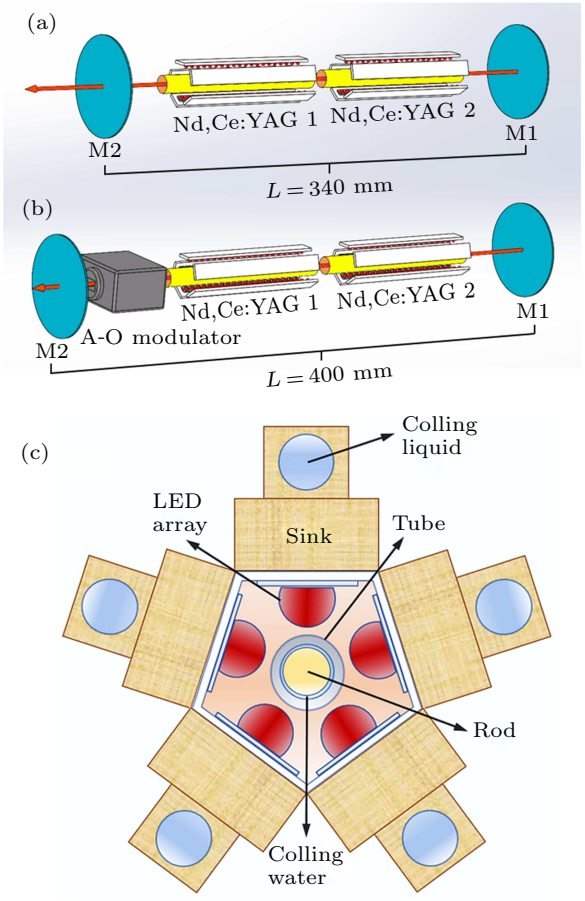


Fig. 1. (a) Experimental setup of CW LED-pumped two-rod Nd,Ce:YAG laser oscillator with $L = 340$ mm, (b) setup for the A-O Q-switched operation with $L = 400$ mm, (c) cross-sectional schematic diagram of fivefold symmetric LED pump module.

3. Results and discussion

The spectral overlap of the blue LED (Luminus, SST-20-B-450 nm), NIR LED (Luminus, SST-10-NIR-810 nm) and the laser with the normalized transmission of the Nd,Ce:YAG rod are shown in Fig. 2, in which the peak wavelength of the laser exhibits a slight red-shift from 1063.68 nm to 1063.92 nm with the increase of input power. During the contrasting experiment using different pump LEDs emitting either at 450 nm or 810 nm, the single module achieves its maximum output power and optical efficiency under 810 nm pumping, with the Nd,Ce:YAG rod operating at a repetition rate of 100 Hz with a pump duration of 2 ms, as illustrated in Fig. 3. Firstly, due to the full-width-half-maximum (FWHM) of the 810-nm LED emission spectrum with a width of 30 nm, a good match with the transmission spectrum of the Nd,Ce:YAG reduces the quantum defects and increases conversion efficiency. Secondly, based on the good sensitization of Nd^{3+} by Ce^{3+} doped into the YAG crystal, the Nd,Ce:YAG has stronger emission in the near infrared band by 795-nm excitations, corresponding to the range of 810-nm LED emission spectrum, and the energy can be absorbed by Nd^{3+} through the luminescence effect of spontaneous radiation.[18] Thirdly, due to the large divergence (lens angle = 120°) and the low optical power of the blue LED, the laser performance pumping at 450 nm is inferior to that pumping at 810 nm in the QCW regime. In the end, single-module with Nd,Ce:YAG and Nd:YAG rod using

different pump LEDs emitting either at 450 nm or 810 nm cannot achieve CW laser operation due to the high laser oscillating threshold and the low electro–optical conversion efficiency.

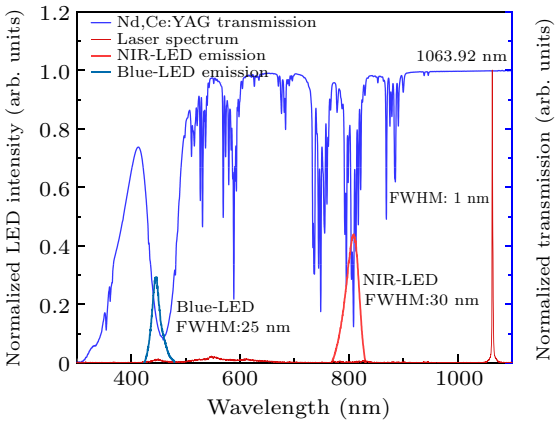


Fig. 2. Spectral overlap of both the LED emission and the laser at 1063.92 nm superimposed on the measured normalized transmission of the Nd,Ce:YAG rod.

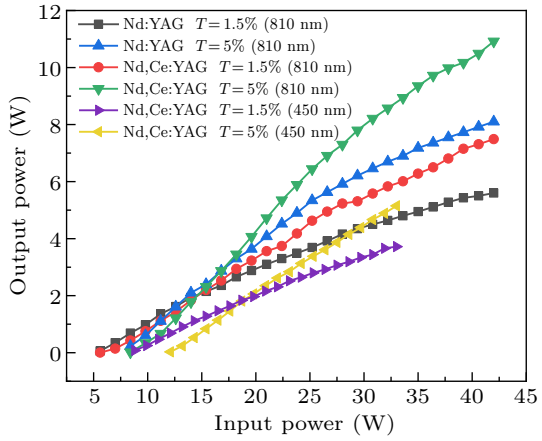


Fig. 3. Comparison of output power between Nd,Ce:YAG and Nd:YAG with a single module under 810 nm and 450 nm in the QCW regime.

According to previous single-module QCW laser performance test data, a CW LED-side-pumped two-rod Nd,Ce:YAG laser structure is designed to reduce the laser oscillating threshold and increase the cavity pump power density. Figure 4 shows the plots of the output power versus input power of the CW laser at 1064 nm for three coupling transmissivities with two identical LED-side-pumped laser modules. Limited by the CW operation of the LED, the coupling output mirror with low transmittance obtains a higher output power. According to the data in Fig. 4, in multi-mode operation, the maximum output power achieved at $T = 1.5\%$@1064 nm is 4.41 W, corresponding to an optical conversion efficiency of 5.3% and a slope efficiency of 12.4%. The threshold pump power for CW operation is 50.4 W, with an incident current of 1.8 A, which is significantly higher than the 5.2-W threshold for QCW operation. The CW laser output power is not yet saturated at various transmissivities, which means that higher transmittance output coupling lenses with more intense pumping can be tried to further improve conversion efficiency by combining effective optimization design of the power supply parameters and cooling structure. In a word, we have achieved the highest average output power and optical conversion efficiency in CW operation at 1064 nm, exceeding all reported LED-pumped CW solid-state laser oscillators.

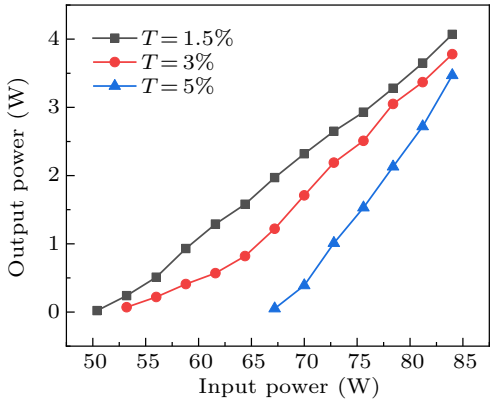


Fig. 4. Plots of 1064-nm output power versus incident power under CW operation.

In comparative experiments with different repetition rates, as the frequency increases, the maximum output average power of the laser increases from 0.15 W to 2.7 W, and the pulse width increases from 406.8 ns to 860.8 ns, while the corresponding peak power significantly decreases, as shown in Fig. 5.

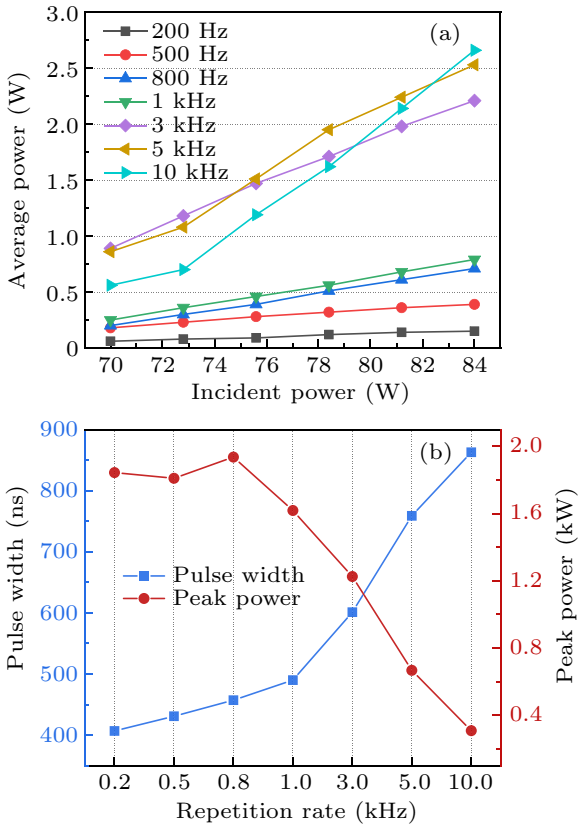


Fig. 5. Plots of (a) average power versus incident pump power at different repetition frequencies A-O modulation and (b) peak power and pulse width versus repetition frequencies.

The optimal output peak power of 1.94 kW for *Q*-switched operation is obtained at a repetition rate of 800 Hz,

corresponding to a single pulse energy of 0.89 mJ with a duration of 457.2 ns. And the maximum average power of 2.7 W is obtained at 10 kHz, corresponding to a single pulse energy of 0.27 mJ with a duration of 860.8 ns. Due to the fact that the pump power density on the cross section of the gain medium is less than 10.7 W/cm^2 (0.42 W$\times$5/0.0625π cm^2), increasing the pump power density can further compress the pulse width and reduce insertion loss.

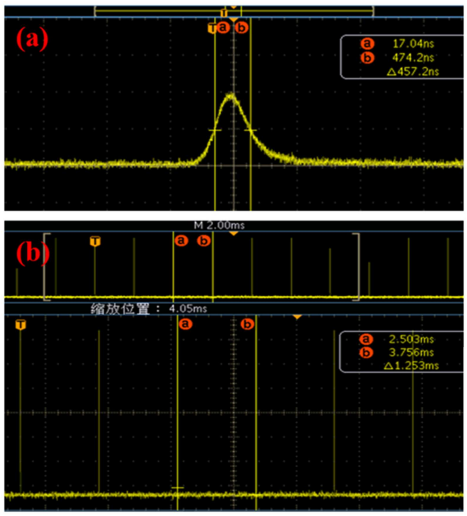


Fig. 6. Single laser pulse at 1064 nm after Q-switch, (b) temporal profile of the pulse sequence at 800 Hz.

Figure 6 displays the measured individual laser pulse and pulse sequences in multi-mode operation at a repetition rate of 800 Hz, which are determined by a high-speed photodiode (Thorlabs. PDA10A2). And the peak-to-peak fluctuation is less than 20%, where the output power oscillations and the amplitude fluctuations are also accompanied by temperature fluctuations during each cooling cycle in this experiment. Figure 7 shows the beam quality measured near the beam waist and far-field energy distribution for CW (see Fig. 7(a)) operation and Q-switched operation (see Fig. 7(b)), which are recorded by the beam analyzer (Cinogy, CMOS-1201). The inserts in Fig. 7 show the intensity profile of the laser beam at the laser waist. The M^2 factor is measured to be about 9.9 for CW operation and 8.8 for Q-switched operation at the highest output power through least-squares curve fitting by the Origin software, respectively.

Figure 8 illustrates the fluctuations of laser output in CW operation, in which the average power data are counted in steps of 0.5 min. After a significant attenuation before the 4-min mark, the output power oscillations are accompanied by temperature fluctuations during each cooling cycle. These fluctuations progressively diminishes after running for 4 min, in which the output power stability root mean square (RMS) is less than 15.7% through the 20-min experiment of stability. And the main influencing factors are that in the peak wavelength of the LED chips emerges the red-shift phenomenon with temperature rising, which can remarkably reduce the pumping efficiency and thus influence the output power stability of CW operation.

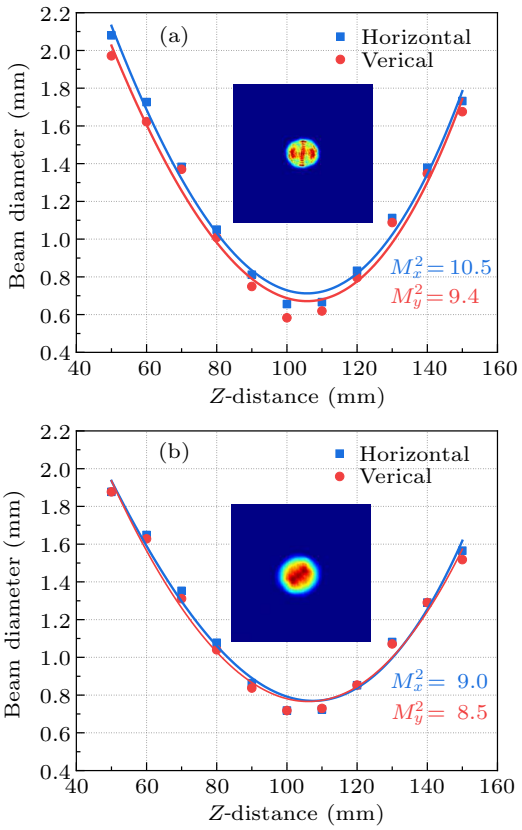


Fig. 7. Beam quality and two-dimensional laser beam profiles of (a) CW and (b) Q-switched operation.

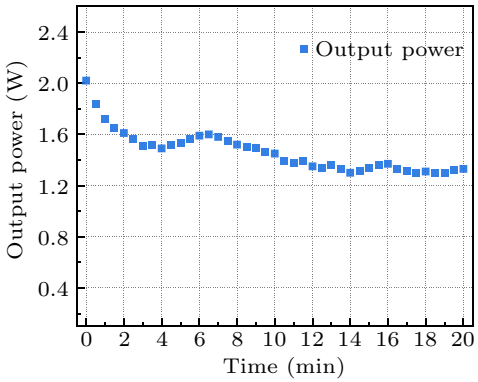


Fig. 8. Stability of laser output in CW operation with medium power in 20 min.

According to the previous output power stability and the beam quality factors of CW operation, the spectral characteristics of the NIR LED with accompanying temporal changes need re-studying and analyzing. Figure 9 shows the superposition of spectra recorded every 10 s for a single LED array driven by QCW current and CW current for 4 min at an initial coolant temperature of 5 °C. Firstly, in both operating modes, the central wavelengths of the LED chips exhibit a red-shift phenomenon simultaneously. As evidenced by the comparison of luminous intensity between Figs. 9(a) and 9(b), CW operation of the LED array generates more waste heat than QCW

operation under the same pump operating conditions, leading to thermally induced spatial variation of the refractive index to increase and the crystal rod to act as a lens with a variable focal length. Secondly, thermal lens dispersion and spherical aberration can cause the stable region of the laser on the meridian plane of the laser resonant cavity to separate from the arc sagittal plane, seriously affecting the output power stability and the beam quality factor of CW operation. The experimental results in Figs. 7 and 8 confirm that the previous theoretical analyses are very good. Finally, with the passage of operating time, due to the intervention of the strong cooling cycles, the phenomena of radiation intensity attenuation and the red shift of peak wavelengths eventually become relatively stable, and the stable range of CW laser operation is in a relatively stable state.

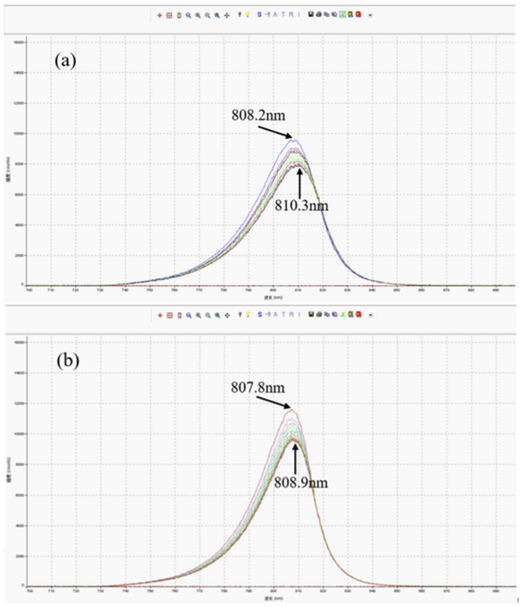


Fig. 9. Superposition of spectra recorded every 10 s during 4-min operation of a single LED array driven by (a) QCW current and (b) CW current respectively.

We estimate the fundamental mode spot radius ω_0 in the primary plane of a single rod through using round-trip ABCD transmission matrix simulations, where the second-order matrix defines the spot radius $\omega_{\rm pm}$ approximated as $(2p+|m|+1)^{1/2}$ times ω_0 with p and m being the radial and angular indices, respectively, as shown in Fig. 10. The radius of higher-order mode, measured in front of the output mirror, is about 2 mm, which is basically consistent with the calculation result. Subsequently, an He–Ne laser beam is collimated to the diameter near the Nd, Ce:YAG rod and injected into the laser rod pumped by the LEDs, as shown in the insert of Fig. 10. The thermal lens focal length can be achieved by measuring the focus point position of the He–Ne laser. And the experimentally measured thermal focal length value is greater than 3 m. Combined with the measured thermal focal length value and theoretical analyses of laser cavity mode, it can be concluded that the marked ranges a and b correspond to the power-stable region and mode-stable region within LED-pumped CW solid-state laser's optimal working stability zone, while the marked mode-stable region c and power-stable region d within the traditional LD-pumped CW solid-state laser are optima work stability zone.[19–25,25] Due to the thermal accumulation from LED CW pumping, the temperature difference between the crystal's interior and thermal distortion gradually increase, resulting in a transition from range a to range b in the laser stable area. Moreover, the value of thermal focal length gradually becomes smaller, and the value of the fundamental mode spot radius ω_0 and mode volume also decreases accordingly. Therefore the LED-pumped CW laser output power will be limited and cannot be further improved. According to the experimental measurement data, observational phenomena, and previous theoretical analyses, it is almost certain that the value of the fundamental mode spot radius ω_0 under LED-pumped CW solid-state laser is 1.5 times or more than that of the conventional LD pumped solid-state cavity structure, which means that the theoretical system of the solid laser cavity mode and the resonant cavity design scheme are further improved and optimized.

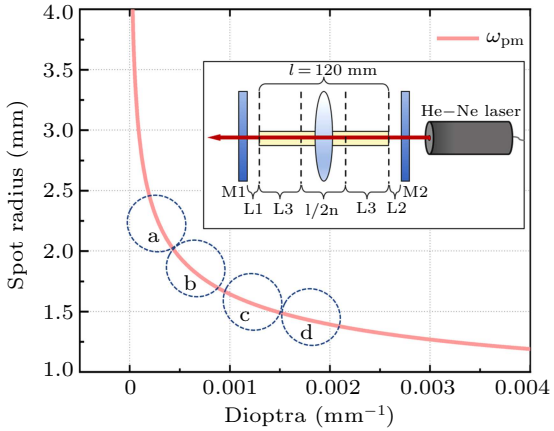


Fig. 10. Spot radius versus diopter in main plane of an equivalent thermal lens in a single module resonator, with insert showing the diagram of single rod construction.

4. Discussion and conclusion

In summary, we have demonstrated a high-performance LED-side-pumped two-rod Nd,Ce:YAG laser with CW operation and Q-switched operation. In the CW regime, the laser achieves a maximum value of output average power of 4.41 W at 1064 nm, corresponding to the highest optical conversion efficiency of 5.3% and a slope efficiency of 12.4%. In the active Q-switched operation, the pulse energy of laser is as high as 0.89 mJ at a repetition rate of 800 Hz with a pulse width of 457.2 ns, corresponding to the highest peak output power of 1.94 kW, and the M^2 factor is measured to be about 8.8. And the main influencing factors are that in the peak wavelength of the LED chips emerges the red-shift phenomenon with a

rise of temperature, which remarkably reduces the pumping efficiency, and thus influencing the output power stability of CW operation. Combined with the measured thermal focal length values and theoretical analyses of laser cavity mode, it is almost certain that the value of the fundamental mode spot radius ω_0 within LED-pumped CW solid-state laser is almost 1.5 times or more than that of the conventional LD pumped solid-state cavity structure. The LED lighting is a dynamic and rapidly evolving field, continuously enhancing the performance of LEDs. We anticipate that LED pumping may rival LD bar pumping in the future.

Acknowledgements

Project supported by the Fund from Nanjing University of Posts and Telecommunications, China (Grant Nos. JUH219002 and JUH219007) and by the Key Research and Development Program of Shandong Province, China (Grant No. 2021CXGC010202).

References

[1] Ochs S A and Pankove J I 1964 *Proc. IEEE* **52** 713
[2] Allen R B and Scalise S J 1969 *Appl. Phys. Lett.* **14** 188
[3] Ostermayer F 1977 *IEEE J. Quantum Electron.* **13** 1
[4] Farmer G I and Kiang Y C 1974 *J. Appl. Phys.* **45** 1356
[5] Saruwatari M and Kimura T 1976 *IEEE J. Quantum Electron.* **12** 584
[6] Stone J, Burrus C A, Dentai A G and Miller B I 1976 *Appl. Phys. Lett.* **29** 37
[7] Huang K Y, Su C K, Lin M W, Chiu Y C and Huang Y C 2016 *Opt. Express* **24** 12043
[8] Lee K, Bae S, Gwag J S, Kwon J H and Yi J 2011 *Korean Phys. Soc.* **59** 3239
[9] Huang W D, Zhao T Z, Xiao H, Zhao S H, Nie S Z, Li X and Zhong Q X 2021 *Optik* **244** 167561
[10] Barbet A, Balembois F, Paul A, Blanchot J P, Viotti A L, Sabater J, Druon F and Georges P 2014 *Opt. Lett.* **39** 6731
[11] Villars B, Steven Hill E and Durfee C G 2015 *Opt. Lett.* **40** 3049
[12] Barbet A, Paul A, Gallinelli T, Balembois F, Blanchot J P, Forget S, Chénais S, Druon F and Georges P 2016 *Optica* **3** 465
[13] Cho C Y, Pu C C, Su K W and Chen Y F 2017 *Opt. Lett.* **42** 2394
[14] Farahbod A and Tarkashvand M 2017 *Iranian Journal of Physics Research* **18** 477
[15] Shen J P, Huang X, Jiang S T, Jiang R R, Wang H Y, Lu P, Xu S C and Jiao M Y 2022 *Chin. Phys. Lett.* **39** 104201
[16] Zhao T Z, Xiao H, Ge W Q, Zhong Q X, Yu J Q, Ming S, Li J and Fan Z W 2019 *Opt. Lett.* **44** 1956
[17] Chiang H, Huang K and Huang Y 2018 *Laser Congress* (ASSL), OSA Technical Digest, AM6A.22
[18] Guo Y W, Huang J Q, Ke G Z, Ma Y Y, Quan J L and Yi G B 2021 *Journal of Luminescence* **236** 118134
[19] Bo Y, Geng A C, Bi Y, Sun Z P, Yang X D, Peng Q J, Li H Q, Li R N, Cui D F and Xu Z Y 2005 *Chin. Phys. B* **14** 771
[20] Song Z X, Bian Q, Shen Y, Gong K L, Zong N, Zong Q S, Bo Y and Peng Q J 2022 *Chin. Phys. B* **31** 054208
[21] Maleki A, Tehrani M K, Saghafifar H and Moghtader Dindarlu M H 2016 *Chin. Phys. B* **25** 034206
[22] Li X P, Yang J, Zhang M S, Yang T L, Wang X J and Peng Q J 2022 *Chin. Phys. B* **31** 084207
[23] Peng H P, Yang C, Lu S, Ma N and Chen M 2019 *Chin. Phys. B* **28** 024205
[24] Wu M Y, Qu P F, Wang S Y, Guo Z, Cai D and Li B B 2018 *Chin. Phys. B* **27** 094207
[25] Moghtader Dindarlu M H, Kavosh Tehrani1 M, Saghafifar H and Maleki A 2015 *Chin. Phys. B* **24** 124205